JACS
JOURNAL OF THE AMERICAN CHEMICAL SOCIETY
pubs.acs.org/JACS
Article

A Visible and Near-Infrared Light Activatable Diazocoumarin Probe for Fluorogenic Protein Labeling in Living Cells

Sheng-Yao Dai and Dan Yang*

Cite This: J. Am. Chem. Soc. 2020, 142, 17156−17166
Read Online

ABSTRACT: Chemical modification of proteins in living cells permits valuable glimpses into the molecular interactions that underpin dynamic cellular events. While genetic engineering methods are often preferred, selective labeling of endogenous proteins in a complex intracellular milieu with chemical approaches represents a significant challenge. In this study, we report novel diazocoumarin compounds that can be photoactivated by visible (430−490 nm) and near-infrared light (800 nm) irradiation to photo-uncage reactive carbene intermediates, which could subsequently undergo an insertion reaction with concomitant fluorescence "turned on". With these new molecules in hand, we have developed a new approach for rapid, selective, and fluorogenic labeling of endogenous protein in living cells. By using CA-II and eDHFR as model proteins, we demonstrated that subcellular localization of proteins can be precisely visualized by live-cell imaging and protein levels can be reliably quantified in multiple cell types using flow cytometry. Dynamic protein regulations such as hypoxia-induced CA-IX accumulation can also be detected. In addition, by two-photon excitation with an 800 nm laser, cell-selective labeling can also be achieved with spatially controlled irradiation. Our method circumvents the cytotoxicity of UV light and obviates the need for introducing external reporters with "click chemistries". We believe that this approach of fluorescence labeling of endogenous protein by bioorthogonal photoirradiation opens up exciting opportunities for discoveries and mechanistic interrogation in chemical biology.

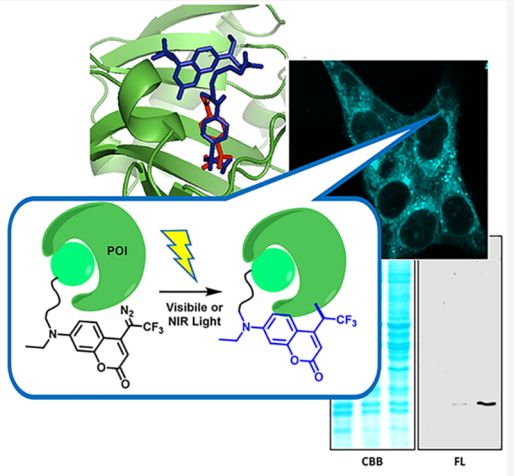

INTRODUCTION

Chemical modification of proteins is a powerful method for protein engineering and conjugation to construct biopharmaceuticals.[1−3] The ability to selectively label proteins, particularly in living cells, is critical for characterizing protein function, localization, and dynamics but is challenging for chemical biology and drug development.[4−7] Precise protein labeling can be achieved by genetic engineering approaches, such as fusion with fluorescent proteins, self-labeling tags[8] (e.g., SNAP-tag,[9] CLIP-tag,[10] and HaloTag[11]), or incorporation of unnatural amino acids (UAAs) by amber codon suppression.[12] However, the considerably large fusion proteins (19−33 kDa) may perturb the functions of POIs. The challenges of UAA incorporation in mammalian cells also hindered its wide applications.[13] Most importantly, these methods can only be applied to cell types that are amenable to genetic manipulation. Direct chemical modification of endogenous proteins with small molecules is a prevailing avenue, as it minimally perturbs protein functions because of the small sizes and bypasses the need for genetic manipulation. However, small-molecule-based live-cell protein labeling was only achieved by limited examples including ligand-directed chemistry developed by the Hamachi group and others.[14−19] Their strategies rely on nucleophilic residues on proteins to react with the electrophilic moiety of affinity-based probes, which may intrinsically compromise the labeling efficiency due to restricted amino acid coverage and competing hydrolysis reaction. Developing new chemistries for selective modification of native endogenous proteins has thus become one of the most important challenges.

Carbene-mediated insertion reactions have been demonstrated to be versatile methods in protein labeling because of their ability to modify a broad scope of residues. One of the most well-known carbene precursors are diazo compounds, which have recently been employed extensively in chemical biology.[20] For instance, it has been demonstrated that purified peptides or proteins can be labeled *in vitro* by metallocarbenoid with the use of dirhodium(II)−metallopeptides[21−29] and ruthenium(II)−porphyrin[30] catalysts. Reactive carbene intermediates can also be photochemically generated

Received: July 27, 2020
Published: September 1, 2020

https://dx.doi.org/10.1021/jacs.0c08068
J. Am. Chem. Soc. 2020, 142, 17156−17166

from diazo and diazirine compounds to label proteins in cells for photoaffinity protein profiling.[31] However, their activation requires UV irradiation that is detrimental to biomolecules and cells via DNA damage[32−34] and generation of reactive oxygen species,[35] which hindered the subsequent live-cell applications. How to design new diazo compounds for specific protein modification in live cells in a bioorthogonal manner is still challenging.

Here we present a new photochemical approach by connecting a diazo group to an extended π conjugation system, such as a fluorophore, which allows the excitation wavelength of the diazo group to be drastically red-shifted from 254 nm[36,37] to the visible light region and enables specific intracellular protein labeling in a biocompatible manner without click chemistry (Scheme 1a). Such a protein modification strategy presents several advantages. First, compared to methods utilizing diazirine,[38,39] benzophenone,[40] aryl azide,[41−44] tetrazole,[45−50] and α-ketoamide,[51] the use of long-wavelength (400−800 nm) irradiation can avoid the cytotoxicity of UV light. Second, copper(I)-catalyzed azide−alkyne cycloaddition (CuAAC) or other reactions that are often required to introduce fluorescence reporters can be obviated, which allows a real-time report of labeled proteins. Furthermore, the photochemical method provides rapid and noninvasive controls for labeling with spatiotemporal precision.[52−55]

Scheme 1. (a) Schematic Illustration of Light-Induced Fluorogenic Labeling of the Protein of Interest (POI); (b) Photoinduced Carbene Insertion Reaction of Diazocoumarins 1 and 2

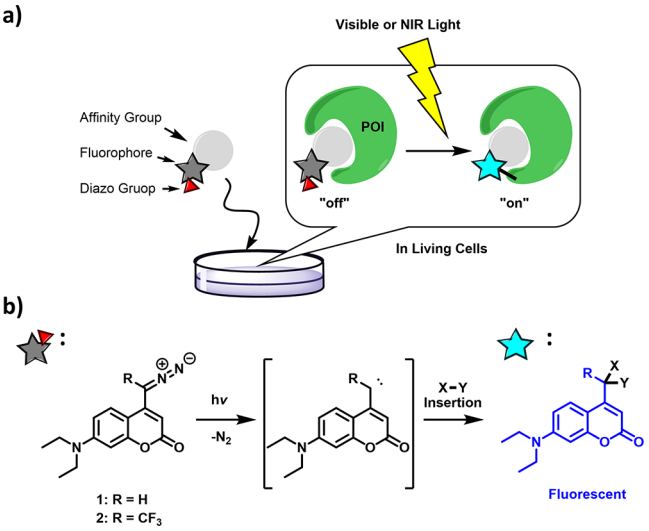

In our studies, we first analyzed the photolysis reaction of diazocoumarins under visible light irradiation and further optimized the structure by introducing a trifluoromethyl substituent adjacent to the diazo group to improve the carbene insertion propensity. Covalent modification of purified proteins by diazocoumarin can be accomplished with mild irradiation of blue LED lamps. It was confirmed that a range of amino acids can be covalently modified. Directed by small-molecule ligands, labeling of specific proteins was further advanced into living cells. Notably, the protein labeling in cells was found to be rapid, mild, and specific. The coumarin fluorescence was recovered upon photoirradiation to facilitate the instant report of labeled proteins in a variety of analyses, including SDS-PAGE, confocal microscopy, and flow cytometry. Furthermore, *in situ* two-photon labeling was achieved in cells with a near-infrared laser, providing an exciting potential for achieving protein labeling with spatiotemporal control. Collectively, we envision that diazocoumarin probes can be exploited as a new photochemical tool for live-cell protein modifications to facilitate the future biological studies and also provide useful templates for the rational design of next-generation protein modification reactions.

RESULTS AND DISCUSSION

Photochemical Characterization of Diazocoumarins under Blue Light. In the course of surveying different combinations of diazo group and fluorophores, we found that 4-diazomethylcoumarins[56−59] were used as precursors for photoreleasing of compounds,[60] but the photochemistry of those diazo compounds has been unexplored. We hypothesize that diazocoumarin compounds can be activated by photoirradiation with long-wavelength light to "uncage" reactive carbene species for covalent modification of proximal proteins (Scheme 1b). To test whether diazocoumarins can be photoactivated by visible light, we synthesized compound **1** according to procedures reported in the literature (Scheme S1).[58] It was found that a large portion of the longest absorption peak fell into the visible light region (>400 nm) (Figure S1a). Unlike ordinary coumarins, the fluorescence of **1** was found to be quenched by the diazo group, presumably via internal charge transfer (ICT).[61] Consequently, photolysis of **1** was first performed in methanol by irradiation with a household blue LED lamp (430−490 nm). Upon irradiation, changes in absorption and fluorescence spectra were observed (Figure S1a,b), indicating a photochemical transformation of **1** under blue light as we anticipated. It is highly conceivable that a carbene intermediate is formed and trapped by methanol.

Scheme 2. Photolysis of 2 (30 μM) in Methanol upon Blue LED Irradiation and the Isolated Yields of Photolysis Products

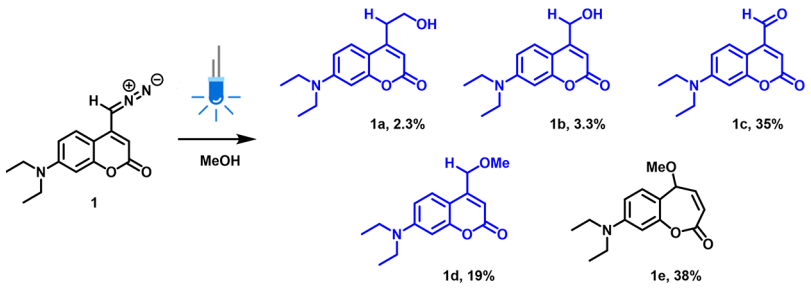

https://dx.doi.org/10.1021/jacs.0c08068
J. Am. Chem. Soc. 2020, 142, 17156−17166

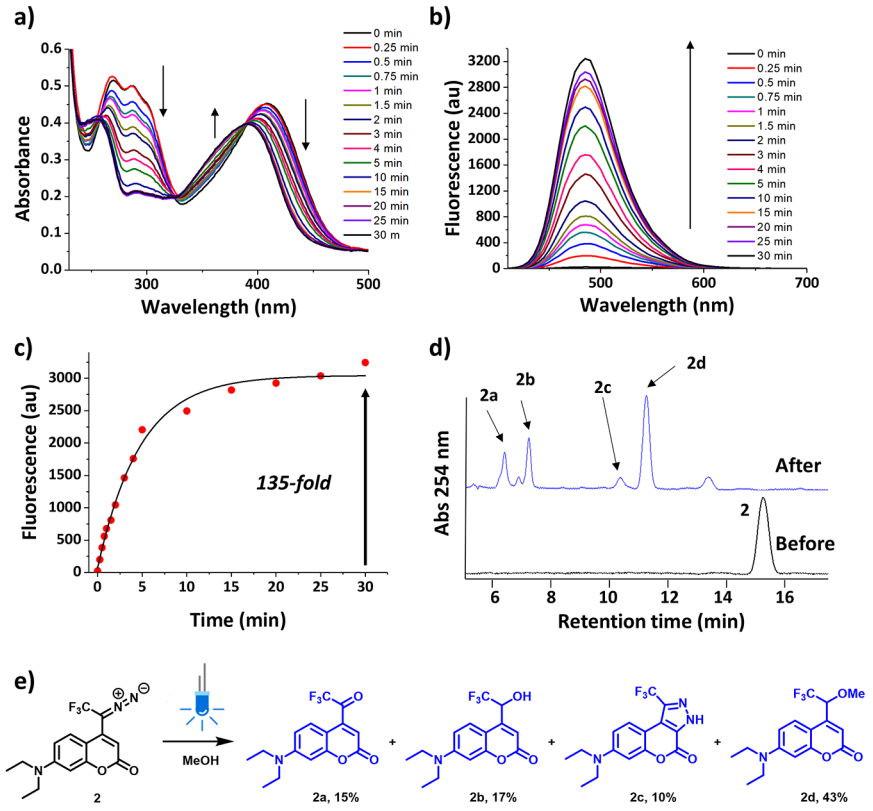

Figure 1. Photochemical characterizations of diazocoumarins. (a, b) Change in absorption and emission spectra of **2** (30 μM) in methanol upon blue LED irradiation. λ_{ex} = 400 nm. (c) Change in fluorescence intensity at λ_{em} = 484 nm upon blue LED irradiation. (d) HPLC analysis of **2** before and after photolysis. (e) Isolated yields of photolysis products.

The reaction mixture was analyzed by LCMS, and multiple products were observed (Figure S1c). To identify these products, a large-scale photolysis reaction was performed. The photolysis mixture was found to include several solvent insertion products (Scheme 2 and Figure S1d), such as the methanol C−H insertion product **1a** (2.3%), the water insertion product **1b** (3.3%), and the methanol O−H insertion product **1d** (19%). While an aldehyde product **1c** resulting from the carbene oxidation by oxygen[62] was isolated in 35% yield, the major product was found to be a nonfluorescent ring expansion product **1e** (38%),[63] formed by Wolff rearrangement of the carbene intermediate to an allene[64] followed by methanol addition. This process is undesirable since the allene intermediate has a long lifetime and preferentially reacts with nucleophiles to give nonfluorescent products.

Because the trifluoromethyl substituent can prevent intramolecular rearrangement of the carbene intermediate generated from trifluoromethylaryldiazirine,[65] we designed and synthesized a trifluoromethyl analogue **2** (Scheme S2). Compound **2** was found to have a longer absorption maximum positioned at 408 nm (extinction coefficient ε of 2259 M^{-1} cm^{-1}, Table S1) and was nonfluorescent (quantum yield Φ_{fl} of 0.003). When **2** was subjected to blue LED irradiation, the peak at 408 nm only underwent a slight blue-shift and that at ~300 nm dropped sharply. This indicates the coumarin chromophore was preserved, whereas the diazo moiety that usually absorbs below 300 nm underwent decomposition. A significant fluorescence enhancement of 135-fold was also detected (Figure 1b,c). Subsequent analyses (Figure 1d,e) revealed that most products were fluorescent, including insertion products **2b** (17%) and **2d** (43%, Φ_{fl} of 0.22), ketone product **2a** (15%), and cyclized[66] byproduct **2c** (10%) (Figure S2 and Table S1). Most importantly, no ring expansion was found.

Reactivity and Stability of Diazocoumarins in Biologically Relevant Conditions. Encouraged by these results, we performed the blue-light-prompted reaction of the model protein bovine serum albumin (BSA) with **1** or **2**. The fluorogenic property of coumarin facilitated the visualization of proteins during in-gel fluorescence scanning without the need for "click" chemistry. While both compounds can covalently label BSA at high concentrations, **2** appeared to be more efficient (Figure 2a) than **1**. Through tryptic digestion and tandem mass spectrometry (LC/MS/MS) analysis (Figure 2b,c and Figure S3), 35 and 8 modification sites by **1** and **2** were identified on BSA, respectively. It was found that although the two compounds modified similar regions, **2** labeled neutral and polar side chains without strong preference, suggesting the formation of a reactive carbene intermediate. However, **1** additionally reacted with a large number of nucleophilic residues, such as His, Lys, Ser, Arg, Thr, and Tyr, indicative of the generation of ketene intermediate along with the reactive carbene, which could potentially lead to nonspecific labeling[67] in a more complex environment. These results suggested that **2** is superior to **1** in terms of sensitivity and selectivity in protein labeling. Because diazo groups are prone to decomposition, especially toward thiols[68] and acids,[69] the stability of **2** was further examined. When **2** was incubated with an equal amount of reduced glutathione (GSH), an intracellularly abundant nucleophile and reductant, in

https://dx.doi.org/10.1021/jacs.0c08068
J. Am. Chem. Soc. 2020, 142, 17156−17166

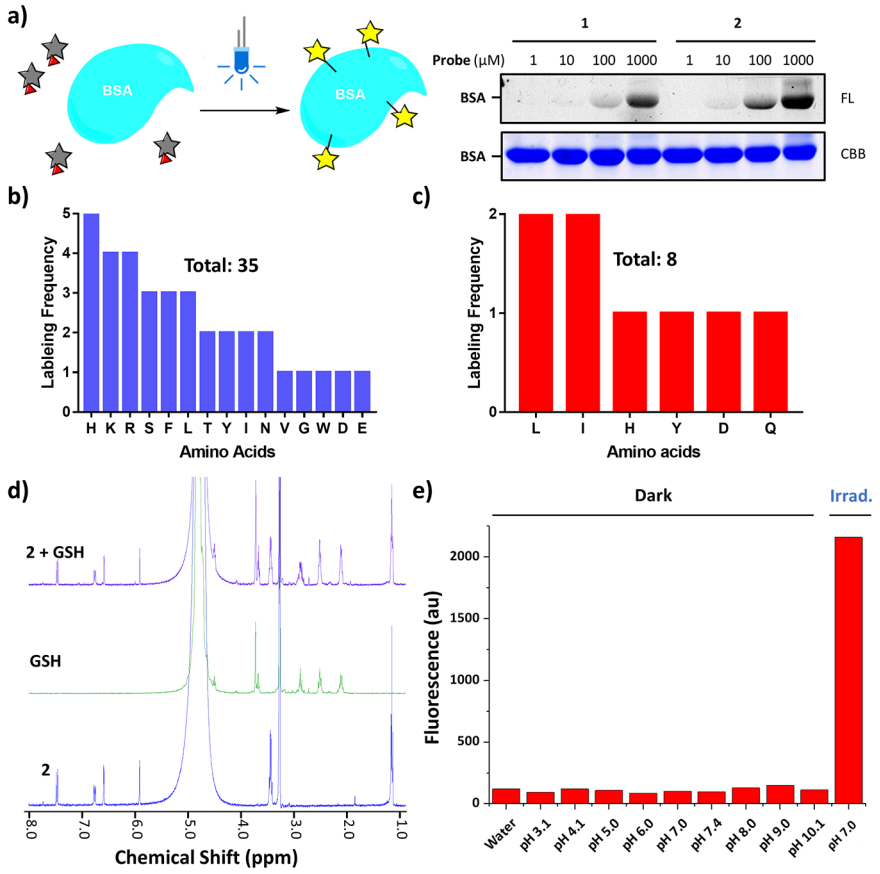

Figure 2. Reactivity and stability of diazocoumarins. (a) SDS-PAGE of BSA (15 μM) labeled by **1** and **2** of various concentrations. (b, c) Bar chart showing the amino acid labeling frequencies of **1** and **2** obtained from tryptic peptide LC/MS/MS analysis of BSA. (d) Comparison of ^{1}H NMR spectra of **2** (5 mM) before and after 24 h incubation in sodium phosphate buffer (10 mM), pH 7.4 (D_2O)/CD_3OD 1:1, in the dark at room temperature, in the presence of reduced glutathione (5 mM). (e) Fluorescence intensity of **2** (λ_{ex} = 400 nm, λ_{em} = 510 nm) in sodium phosphate buffer of various pH values incubated in the dark or under blue LED irradiation as indicated.

phosphate buffer for 24 h in dark, no reaction was observed by NMR analysis (Figure 2d). In addition, as shown in Figure 2e, **2** was stable across a wide range of pH; the fluorescence increased only when the compound was exposed to light.

Labeling of Recombinant CA-II with Blue Light. The affinity-based approach was then employed to achieve specific protein labeling by using small-molecule ligands. Carbonic anhydrase-II (CA-II, 29 kDa) was chosen as a target for selective labeling as it has been widely adopted in studies of affinity-based probes.[70] CA-II can be reversibly inhibited by aromatic primary sulfonamides,[71] such as 4-carboxybenzenesulfonamide (CBS) (K_d ~ 3.2 μM).[72] Accordingly, we designed and synthesized **3** (Figure 3a and Scheme S2) by modifying one of the ethyl substituents on the 7-amino group to connect CBS through a simple amide linker. *In vitro* labeling of recombinant CA-II was then performed by mixing with **3** followed by blue LED irradiation (Figure 3b). As visualized by the resulting SDS-PAGE, labeling of CA-II by **3** was furnished in both a concentration (Figure 3c, EC_{50}: 2.48 μM) and time (Figure 3d) dependent manner and was diminished by competition with an excess of CBS (Figure 3e, IC_{50}: 182 μM). An enzyme activity assay was performed, which showed that **3** has an IC_{50} value comparable to that of CBS (Figure 3f; IC_{50} of **3**: 0.90 μM; IC_{50} of CBS: 2.14 μM). These results showed that the binding property of the sulfonamide was not disrupted despite its modest interaction with CA-II. In addition, LC/MS/MS analysis revealed that **3** labeled His2 and Trp4 residues of the *N*-terminal peptide of CA-II (Figure 3g and Figure S4). Both residues were located at the entrance of the ligand-binding pocket (Figure 3h), suggesting that labeling is induced by the specific interaction between CA-II and **3**. Consistently, exclusive labeling of 29 kDa CA-II could also be observed in HeLa cell lysates spiked with the recombinant protein (Figure S5a).

Labeling of Endogenous CA-II in Living Cells. Our ultimate goal is to label endogenously expressed proteins in living cells. Therefore, labeling was attempted with live MCF7 human breast cancer cells[73] and HCT116 human colorectal cancer cells,[74] which endogenously express CA-II. After incubation with **3**, cells were irradiated with the blue LED lamp (Figure 4a). Subsequently, cell lysates were harvested and separated by SDS-PAGE to visualize the fluorescent signal. A strong single fluorescent band corresponds to CA-II was observed in SDS-PAGE of MCF7 cells but was blocked by CBS cotreatment (Figure 4b, lanes 3 and 4). A weaker band was observed without irradiation (Figure 4b, lane 2), suggesting that a minor reaction occurred in the dark. Western blot analysis confirms that CA-II was evenly expressed among the four groups and matched the molecular weight of fluorescent bands. Similar results were obtained in HCT116 cells (Figure S5b,c). Surprisingly, in the live-cell time-dependent experiments, the labeling was found to complete

https://dx.doi.org/10.1021/jacs.0c08068
J. Am. Chem. Soc. 2020, 142, 17156−17166

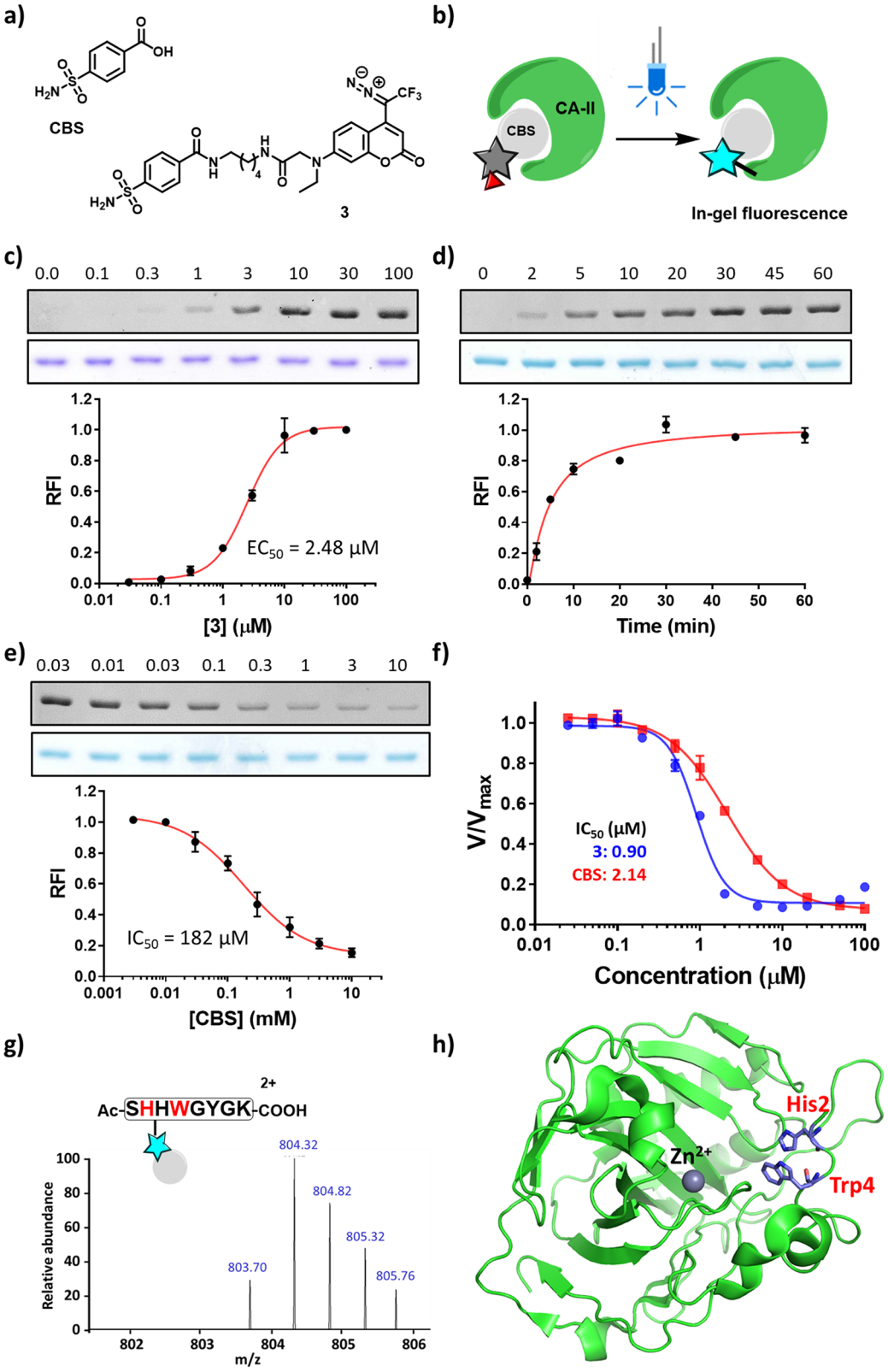

Figure 3. Fluorescence labeling of recombinant CA-II with blue light. (a) Structures of 4-carbonxybenzenesulfonamide (CBS) and **3**. (b) Schematic illustration of blue LED light-induced labeling of recombinant CA-II. (c–e) SDS-PAGE of recombinant CA-II (1.7 μM) labeled by **3** (10 μM in (d) and (e)) under blue LED irradiation. (f) Enzymatic activity assay of CA-II catalyzed the hydrolysis of *p*-nitrophenyl acetate. Error bar indicates SD, n = 3. (g) Mass spectrum of modified CA-II tryptic peptide by **3**. (h) Crystal structure of CA-II showing Zn^{2+} ion and the two labeled residues.

https://dx.doi.org/10.1021/jacs.0c08068
J. Am. Chem. Soc. 2020, 142, 17156–17166

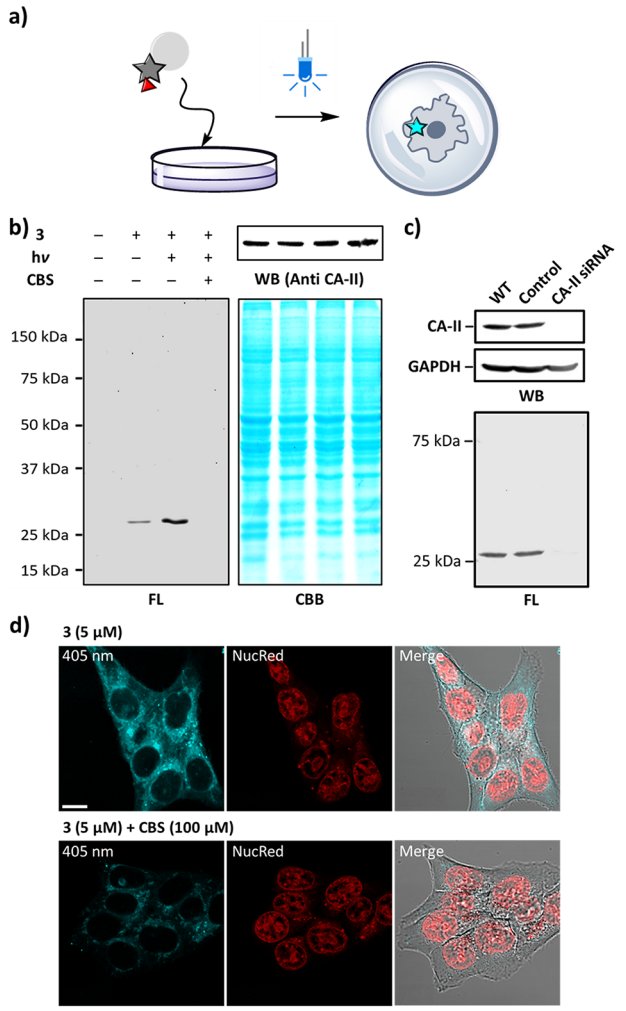

Figure 4. Fluorescence labeling of endogenously CA-II in cells. (a) Schematic illustration of live-cell labeling. (b) SDS-PAGE of MCF7 live-cell labeling by **3** (10 μM) in the presence/absence of CBS (200 μM). (c) SDS-PAGE and Western blot of MCF7 live-cell labeling by **3** (10 μM) after CA-II knockdown by siRNA. (d) Live-cell confocal imaging of HCT116 cells treated with **3** (5 μM), followed by blue LED irradiation. **3**: λ_{ex} = 405 nm, NucRed: λ_{ex} = 633 nm. Scale bar = 10 μm.

within 2 min under irradiation (Figure S5d). The faster labeling in living cells is presumably attributed to the enriched concentrations of **3** and the intracellular proteins when confined within cells. When the CA-II expression of MCF7 cells was knocked down by siRNA, the in-gel fluorescent signal disappeared (Figure 4c). Taken altogether, these results convincingly demonstrated the visible-light-induced specific and rapid labeling of CA-II by diazocoumarin in living cells.

Because of the unique fluorogenic property of the diazocoumarin probe **3** and biocompatibility of the labeling condition, live-cell imaging of the intracellular CA-II can be performed, which is otherwise difficult to achieve with other methods. After the treatment of **3** with blue LED irradiation, strong fluorescence was observed in the cytosolic region of HCT116 cells (Figure 4d) and MCF7 cells (Figure S6a). In addition, the fluorescent signal was diminished when CBS was added to compete with **3**. When a washout step was performed prior to the irradiation, minimal labeling was observed (Figure S6b). The fluorescence signals were clearly excluded from the nucleus that was stained by the red nucleus probe (NucRed), which was consistent with the reported cytosolic distribution of CA-II.[75] Immunofluorescence staining showed that the signal from **3** was highly colocalized with that of CA-II antibody (Figure S6c). Moreover, the fact that the fluorescence signal of **3** was retained after cell permeabilization is also evidence that the covalent bonding was established in response to light.

By use of fluorescence-activated cell sorting (FACS) analysis, the fluorescence "turn-on" effect and competition can be quantitatively assessed (Figure 5a). As recent work has

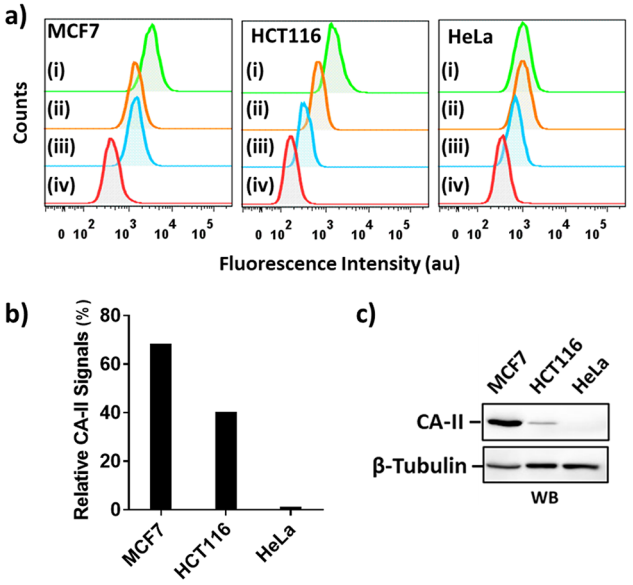

Figure 5. FACS analysis of CA-II expression in different cell types. (a) FACS analysis of cells treated with (i) **3** (5 μM), blue LED irradiation; (ii) **3** (5 μM) and CBS (100 μM), blue LED irradiation; (iii) **3** (5 μM), no irradiation; (iv) untreated. (b) Relative CA-II signals obtained from FACS analysis in MCF7, HCT116, and HeLa cells. (c) Western blot of CA-II in three cell lines.

demonstrated the assessment of the expression level of the cannabinoid receptors by tandem live-cell photoaffinity labeling and click chemistry on fixed cells,[76] we envisage that such an assessment can be performed in living cells with our approach. As shown in Figure 5b, the strongest specific labeling for CA-II was obtained in MCF7 cells, followed by HCT116 cells, whereas HeLa cells showed minimal labeling. This result suggests that the expression level of CA-II should follow this order: MCF7 > HCT116 > HeLa, which was validated by Western blot analysis (Figure 5c).

Labeling of CA-IX under Hypoxia-Mimetic Conditions. CA-IX is a membrane-associated isoform of CAs, which is markedly overexpressed in hypoxic tumor cells.[77] As it plays a pivotal role in malignant progression, especially in regulating pH homeostasis under acidic extracellular matrix, CA-IX is thus regarded as a valuable biomarker as well as an attractive target in cancer therapy.[78] The expression of CA-IX is modulated by hypoxia-inducible factor 1 (HIF-1), which under normoxia conditions is hydroxylated at proline residues by prolyl hydroxylase domain-containing protein 2 (PHD2) and subsequently ubiquitinated by Von Hippel–Lindau (VHL) E3 ligase for proteasome degradation (Figure 6a).[79] Because oxygen sensing of PHD2 relies on its catalytic iron(II)

https://dx.doi.org/10.1021/jacs.0c08068
J. Am. Chem. Soc. 2020, 142, 17156−17166

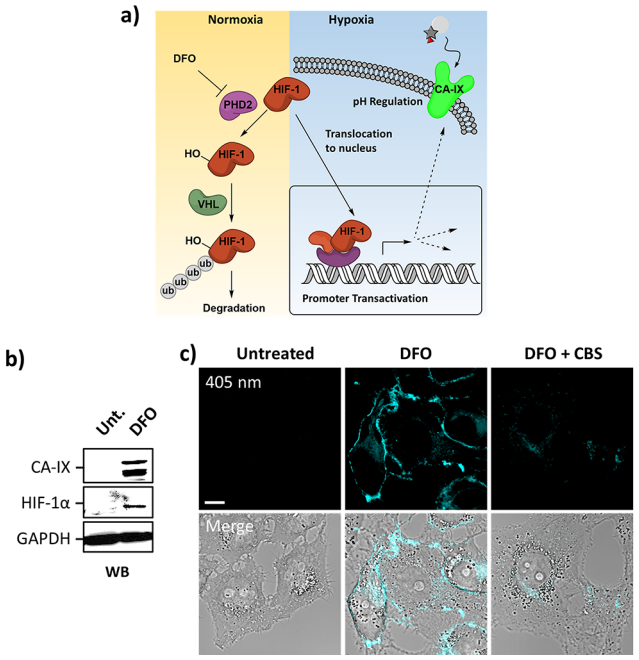

Figure 6. Fluorescence labeling of CA-IX in cells under hypoxia-mimetic conditions. (a) Schematic illustration of inducible CA-IX expression under hypoxia or treatment by DFO. (b) Western blot of HeLa cells cultured under normal or hypoxia-mimetic (DFO, 100 μM for 24 h) conditions. (c) Live-cell confocal imaging of HeLa cells cultured under normal or hypoxia-mimetic (DFO, 100 μM for 24 h) conditions. Cells were treated with **3** (5 μM) in the presence/absence of CBS (100 μM), followed by blue LED irradiation. **3**: λ_{ex} = 405 nm. Scale bar = 10 μm.

center, iron chelator deferoxamine mesylate (DFO) can inhibit PHD2 to stabilize HIF-1, thus acting as a hypoxia-mimetic agent.[80] In our experiment, HeLa cells, which have no CA-II expression, were cultured under normal or hypoxia-mimetic conditions (treated with DFO). From the Western blot result shown in Figure 6b, it can be observed that CA-IX was upregulated as a result of HIF-1 accumulation. After that, these cells were treated with **3** and followed by irradiation with blue LED light. The resulting live-cell confocal images showed that substantial signals accumulated on the plasma membrane in cells treated with DFO, while untreated cells displayed minimal signal (Figure 6c). The majority of the signals could be displaced by cotreatment of CBS. This evidently indicated that **3** could fluorescently label the membrane-bound CA-IX under hypoxia-mimetic conditions. Our results demonstrated that our visible light activated probe could be used for labeling proteins that are dynamically expressed under specific conditions, which is otherwise hard to be accomplished with overexpression system of the genetic modification approach.

***In Situ* Two-Photon Labeling and Imaging.** Because 7-aminocoumarin has been applied in two-photon uncaging,[81] we wonder whether two-photon protein labeling can be performed. In principle, the ability of two-photon activation would potentially lead to reduced phototoxicity, better spatial control, and deeper tissue penetration.[82] We, therefore, tested the feasibility of two-photon activation of **2** to form carbene with the use of near-infrared (NIR) light to initiate the reaction.[83,84] When **2** was exposed to the femtosecond pulses of an 800 nm focused laser beam, a similar photochemical response to that of blue light irradiation was observed (Figure 7a). Dependence of the fluorescence increase on the focused laser power was recorded; however, no reaction occurred when

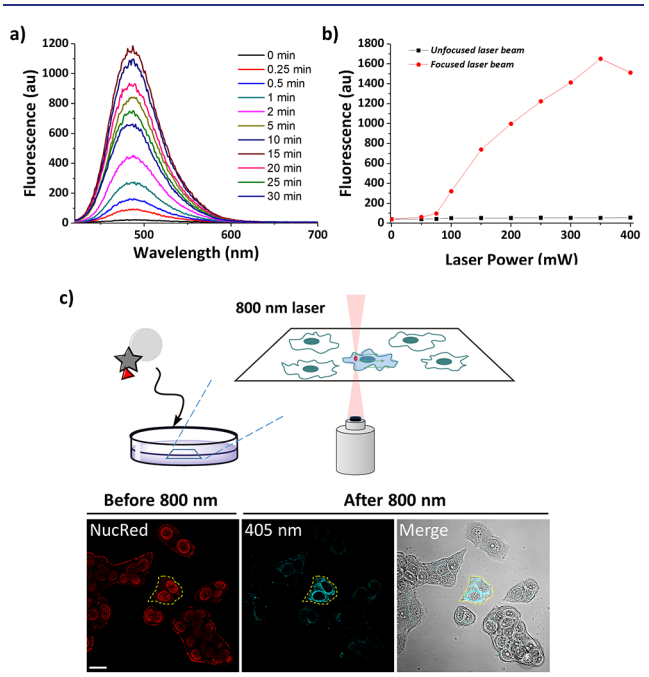

Figure 7. *In situ* two-photon labeling and imaging of CA-II. (a) Change in emission spectra of **2** (30 μM) upon two-photon photolysis with a mode-locked Ti:sapphire 800 nm femtosecond pulses focused laser at 200 mW. Emission was measured at λ_{ex} = 400 nm. (b) Fluorescence intensity (λ_{ex} = 400 nm, λ_{ex} = 484 nm) measured at 30 min after irradiation with focused or unfocused laser beam of varying laser power. (c) Schematic illustration of two-photon induced labeling of CA-II with **3** (5 μM) in living cells and confocal imaging of MCF7 cells before and after two-photon activation with 800 nm. Scale bar = 20 μm.

the laser was unfocused (Figure 7b). These results suggest that **2** can be two-photon activated by NIR light. As a proof-of-concept experiment, *in situ* two-photon labeling and imaging of CA-II was performed in living cells with **3** (Figure 7c). In this experiment, MCF7 cells were treated with **3**, and the cell location was first tracked with NucRed under confocal microscopy. Next, only selected cells were irradiated with a laser at 800 nm of the microscope. Followed by the washing of excess probes, the cells were imaged. As shown in Figure 7c, stronger fluorescence signals were detected in cells exposed to NIR light, indicating that two-photon activated labeling of CA-II can be achieved in live cells.

Labeling of EDHFR in Living Cells. To demonstrate that our labeling strategy can be applied to other target proteins, **4** was synthesized by incorporating trimethoprim (TMP, K_d ~ 10 nM) as a ligand moiety (Figure 8a),[85] which can selectively bind *E. coli* dihydrofolate reductase (eDHFR). HeLa cells were transfected plasmid DNA to overexpress eDHFR fused with a red fluorescent protein (mCherry-eDHFR). The transfection of this fusion protein helps to confirm the colocalization with diazocoumarin in living cells under confocal microscopy. When the cells were treated with **4** (5 μM) and irradiated with blue light, colocalization of the probe signal and mCherry was observed in live-cell imaging (Figure 8b). While the cells without transfection did not show any staining, the addition of

https://dx.doi.org/10.1021/jacs.0c08068
J. Am. Chem. Soc. 2020, 142, 17156−17166

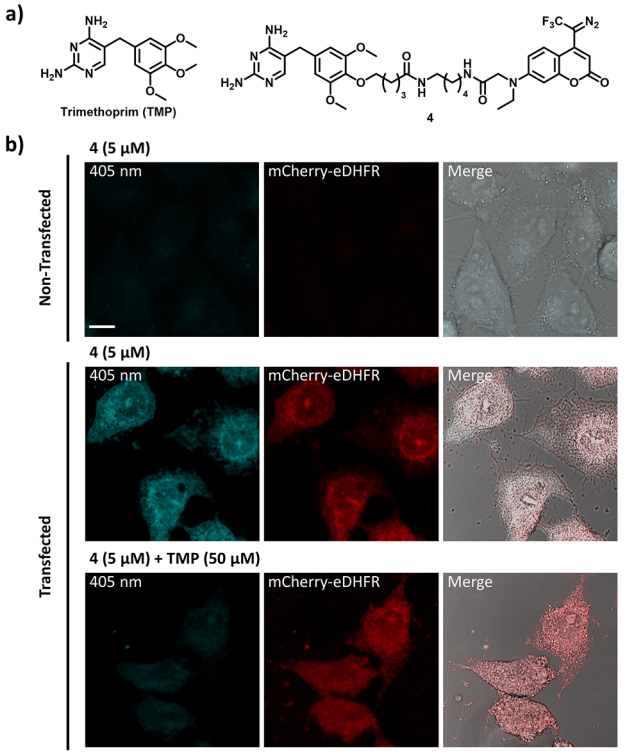

Figure 8. Fluorescence labeling of mCherry-eDHFR in HeLa cells. (a) Chemical structures of TMP and **4**. (b) Live-cell confocal imaging of HeLa cells with or without transient expression of mCherry-eDHFR, treated with **4** (5 μM) and TMP (50 μM) after blue LED irradiation. **4**: λ_{ex} = 405 nm, mCherry: λ_{ex} = 561 nm. Scale bar = 10 μm.

TMP also predictably perturbed the labeling in transfected cells.

CONCLUSION

In the investigation described above, we have demonstrated that diazocoumarin can be activated by visible light to "photo-uncage" reactive carbene intermediate, which can subsequently undergo insertion reaction with biomolecules. Through detailed chemical analysis, the structure of diazocoumarin was optimized by the introduction of a trifluoromethyl group to improve the carbene insertion propensity. Moreover, we showed that efficient visible light photoactivation and fluorogenic property of diazocoumarin can be exploited as a bioorthogonal tool in endogenous protein labeling. As a result, proteins of interest can be covalently modified after mild blue LED irradiation, with instant fluorescence report bypassing the need to perform "click" chemistry. We demonstrated the applications of diazocoumarin in affinity labeling of endogenous proteins in living cells using CA-II as a model protein. Remarkable labeling speed and specificity of endogenous CA-II have been achieved, which enables reliable visualization of localization by live-cell imaging and quantitative assessment of expression level among different cell types by flow cytometry. Live-cell imaging also allowed monitoring of protein dynamics as proved by hypoxia-induced CA-IX accumulation. Furthermore, diazocoumarin can be photoactivated by two-photon excitation, which allows spatiotemporally controlled protein labeling in living cells with the least phototoxic NIR light. As a further illustration, this strategy can also be successfully applied to the labeling of eDHFR. We believe that this photochemical approach should expand the chemical repertoire of the covalent labeling of biomolecules in living cells to facilitate biological discoveries.

ASSOCIATED CONTENT

Supporting Information

The Supporting Information is available free of charge at https://pubs.acs.org/doi/10.1021/jacs.0c08068.

Supporting figures, tables, experimental procedures, synthesis, characterization of compounds, LC/MS/MS spectra, and NMR spectra (PDF)

AUTHOR INFORMATION

Corresponding Author

Dan Yang − *Morningside Laboratory for Chemical Biology, Department of Chemistry, The University of Hong Kong, Hong Kong, China;* orcid.org/0000-0002-1726-9335; Email: yangdan@hku.hk

Author

Sheng-Yao Dai − *Morningside Laboratory for Chemical Biology, Department of Chemistry, The University of Hong Kong, Hong Kong, China*

Complete contact information is available at: https://pubs.acs.org/10.1021/jacs.0c08068

Notes

The authors declare no competing financial interest.

ACKNOWLEDGMENTS

We thank Dr. Ming-De Li (Shantou University) and Prof. David Philip (The University of Hong Kong) for help in the two-photon photolysis experiment setup. We thank Dr. Fang-Fang Shen and Dr. Xiang David Li (The University of Hong Kong) as well as Dr. Nai-Kei Wong (The Second Hospital Affiliated to Southern University of Science and Technology) for helpful advice on experiments and critical reading of the manuscript. We thank The University of Hong Kong Li Ka Shing Faculty of Medicine Faculty Core Facility for support in confocal microscopy and flow cytometry. We thank Dr. Ruijun Tian (Southern University of Science and Technology) for assistance in LC/MS/MS experiment. This work was supported by The University of Hong Kong, the University Development Fund, the Morningside Foundation, and the Hong Kong Research Grants Council under the Area of Excellence Scheme (AoE/P-705/16).

REFERENCES

(1) Hoyt, E. A.; Cal, P. M. S. D.; Oliveira, B. L.; Bernardes, G. J. L. Contemporary approaches to site-selective protein modification. *Nat. Rev. Chem.* **2019**, *3*, 147−171.

(2) Krall, N.; da Cruz, F. P.; Boutureira, O.; Bernardes, G. J. L. Site-selective protein-modification chemistry for basic biology and drug development. *Nat. Chem.* **2016**, *8*, 103−113.

(3) Boutureira, O.; Bernardes, G. J. Advances in chemical protein modification. *Chem. Rev.* **2015**, *115*, 2174−95.

(4) Tamura, T.; Hamachi, I. Chemistry for Covalent Modification of Endogenous/Native Proteins: From Test Tubes to Complex Biological Systems. *J. Am. Chem. Soc.* **2019**, *141*, 2782−2799.

(5) Amaike, K.; Tamura, T.; Hamachi, I. Recognition-driven chemical labeling of endogenous proteins in multi-molecular crowding in live cells. *Chem. Commun.* **2017**, *53*, 11972−11983.

(6) Kubota, R.; Hamachi, I. Protein recognition using synthetic small-molecular binders toward optical protein sensing in vitro and in live cells. *Chem. Soc. Rev.* **2015**, *44*, 4454−71.
(7) Zhang, G.; Zheng, S.; Liu, H.; Chen, P. R. Illuminating biological processes through site-specific protein labeling. *Chem. Soc. Rev.* **2015**, *44*, 3405−17.
(8) Wang, Z.; Ding, X.; Li, S.; Shi, J.; Li, Y. Engineered fluorescence tags for in vivo protein labelling. *RSC Adv.* **2014**, *4*, 7235−7245.
(9) Juillerat, A.; Gronemeyer, T.; Keppler, A.; Gendreizig, S.; Pick, H.; Vogel, H.; Johnsson, K. Directed Evolution of O6-Alkylguanine-DNA Alkyltransferase for Efficient Labeling of Fusion Proteins with Small Molecules In Vivo. *Chem. Biol.* **2003**, *10*, 313−317.
(10) Gautier, A.; Juillerat, A.; Heinis, C.; Corrêa, I. R.; Kindermann, M.; Beaufils, F.; Johnsson, K. An Engineered Protein Tag for Multiprotein Labeling in Living Cells. *Chem. Biol.* **2008**, *15*, 128−136.
(11) Los, G. V.; Encell, L. P.; McDougall, M. G.; Hartzell, D. D.; Karassina, N.; Zimprich, C.; Wood, M. G.; Learish, R.; Ohana, R. F.; Urh, M.; Simpson, D.; Mendez, J.; Zimmerman, K.; Otto, P.; Vidugiris, G.; Zhu, J.; Darzins, A.; Klaubert, D. H.; Bulleit, R. F.; Wood, K. V. HaloTag: A Novel Protein Labeling Technology for Cell Imaging and Protein Analysis. *ACS Chem. Biol.* **2008**, *3*, 373−382.
(12) Lang, K.; Chin, J. W. Cellular incorporation of unnatural amino acids and bioorthogonal labeling of proteins. *Chem. Rev.* **2014**, *114*, 4764−806.
(13) Lin, X.; Yu, A. C.; Chan, T. F. Efforts and Challenges in Engineering the Genetic Code. *Life (Basel, Switz.)* **2017**, *7*, 12.
(14) Tamura, T.; Ueda, T.; Goto, T.; Tsukidate, T.; Shapira, Y.; Nishikawa, Y.; Fujisawa, A.; Hamachi, I. Rapid labelling and covalent inhibition of intracellular native proteins using ligand-directed N-acyl-N-alkyl sulfonamide. *Nat. Commun.* **2018**, *9*, 1870.
(15) Matsuo, K.; Nishikawa, Y.; Masuda, M.; Hamachi, I. Live-Cell Protein Sulfonylation Based on Proximity-driven N-Sulfonyl Pyridone Chemistry. *Angew. Chem., Int. Ed.* **2018**, *57*, 659−662.
(16) Yamaguchi, T.; Asanuma, M.; Nakanishi, S.; Saito, Y.; Okazaki, M.; Dodo, K.; Sodeoka, M. Turn-ON fluorescent affinity labeling using a small bifunctional O-nitrobenzoxadiazole unit. *Chem. Sci.* **2014**, *5*, 1021−1029.
(17) Fujishima, S. H.; Yasui, R.; Miki, T.; Ojida, A.; Hamachi, I. Ligand-directed acyl imidazole chemistry for labeling of membrane-bound proteins on live cells. *J. Am. Chem. Soc.* **2012**, *134*, 3961−4.
(18) Tsukiji, S.; Miyagawa, M.; Takaoka, Y.; Tamura, T.; Hamachi, I. Ligand-directed tosyl chemistry for protein labeling in vivo. *Nat. Chem. Biol.* **2009**, *5*, 341−3.
(19) Hughes, C. C.; Yang, Y.-L.; Liu, W.-T.; Dorrestein, P. C.; Clair, J. J. L.; Fenical, W. Marinopyrrole A Target Elucidation by Acyl Dye Transfer. *J. Am. Chem. Soc.* **2009**, *131*, 12094−12096.
(20) Mix, K. A.; Aronoff, M. R.; Raines, R. T. Diazo Compounds: Versatile Tools for Chemical Biology. *ACS Chem. Biol.* **2016**, *11*, 3233−3244.
(21) Ohata, J.; Ball, Z. T. A Hexa-rhodium Metallopeptide Catalyst for Site-Specific Functionalization of Natural Antibodies. *J. Am. Chem. Soc.* **2017**, *139*, 12617−12622.
(22) Martin, S. C.; Vohidov, F.; Wang, H.; Knudsen, S. E.; Marzec, A. A.; Ball, Z. T. Designing Selectivity in Dirhodium Metallopeptide Catalysts for Protein Modification. *Bioconjugate Chem.* **2017**, *28*, 659−665.
(23) Vohidov, F.; Coughlin, J. M.; Ball, Z. T. Rhodium(II) metallopeptide catalyst design enables fine control in selective functionalization of natural SH3 domains. *Angew. Chem., Int. Ed.* **2015**, *54*, 4587−91.
(24) Minus, M. B.; Liu, W.; Vohidov, F.; Kasembeli, M. M.; Long, X.; Krueger, M. J.; Stevens, A.; Kolosov, M. I.; Tweardy, D. J.; Sison, E. A. R.; Redell, M. S.; Ball, Z. T. Rhodium(II) Proximity-Labeling Identifies a Novel Target Site on STAT3 for Inhibitors with Potent Anti-Leukemia Activity. *Angew. Chem., Int. Ed.* **2015**, *54*, 13085−13089.
(25) Kundu, R.; Ball, Z. T. Rhodium-catalyzed cysteine modification with diazo reagents. *Chem. Commun.* **2013**, *49*, 4166−8.
(26) Chen, Z.; Vohidov, F.; Coughlin, J. M.; Stagg, L. J.; Arold, S. T.; Ladbury, J. E.; Ball, Z. T. Catalytic protein modification with dirhodium metallopeptides: specificity in designed and natural systems. *J. Am. Chem. Soc.* **2012**, *134*, 10138−45.
(27) Popp, B. V.; Ball, Z. T. Proximity-driven metallopeptide catalysis: Remarkable side-chain scope enables modification of the Fos bZip domain. *Chem. Sci.* **2011**, *2*, 690−695.
(28) Chen, Z.; Popp, B. V.; Bovet, C. L.; Ball, Z. T. Site-specific protein modification with a dirhodium metallopeptide catalyst. *ACS Chem. Biol.* **2011**, *6*, 920−5.
(29) Popp, B. V.; Ball, Z. T. Structure-Selective Modification of Aromatic Side Chains with Dirhodium Metallopeptide Catalysts. *J. Am. Chem. Soc.* **2010**, *132*, 6660−6662.
(30) Ho, C.-M.; Zhang, J.-L.; Zhou, C.-Y.; Chan, O.-Y.; Yan, J. J.; Zhang, F.-Y.; Huang, J.-S.; Che, C.-M. A Water-Soluble Ruthenium Glycosylated Porphyrin Catalyst for Carbenoid Transfer Reactions in Aqueous Media with Applications in Bioconjugation Reactions. *J. Am. Chem. Soc.* **2010**, *132*, 1886−1894.
(31) Ge, S.-S.; Chen, B.; Wu, Y.-Y.; Long, Q.-S.; Zhao, Y.-L.; Wang, P.-Y.; Yang, S. Current advances of carbene-mediated photoaffinity labeling in medicinal chemistry. *RSC Adv.* **2018**, *8*, 29428−29454.
(32) Ridley, A. J.; Whiteside, J. R.; McMillan, T. J.; Allinson, S. L. Cellular and sub-cellular responses to UVA in relation to carcinogenesis. *Int. J. Radiat. Biol.* **2009**, *85*, 177−95.
(33) McMillan, T. J.; Leatherman, E.; Ridley, A.; Shorrocks, J.; Tobi, S. E.; Whiteside, J. R. Cellular effects of long wavelength UV light (UVA) in mammalian cells. *J. Pharm. Pharmacol.* **2008**, *60*, 969−76.
(34) Barlev, A.; Sen, D. DNA's Encounter with Ultraviolet Light: An Instinct for Self-Preservation? *Acc. Chem. Res.* **2018**, *51*, 526−533.
(35) Bai, X.; Huang, Y.; Lu, M.; Yang, D. HKOH-1: A Highly Sensitive and Selective Fluorescent Probe for Detecting Endogenous Hydroxyl Radicals in Living Cells. *Angew. Chem., Int. Ed.* **2017**, *56*, 12873−12877.
(36) Chowdhry, V.; Vaughan, R.; Westheimer, F. H., 2-diazo-3,3,3-trifluoropropionyl chloride: reagent for photoaffinity labeling. *Proc. Natl. Acad. Sci. U. S. A.* **1976**, *73*, 1406−1408.
(37) Singh, A.; Thornton, E. R.; Westheimer, F. H. The Photolysis of Diazoacetylchymotrypsin. *J. Biol. Chem.* **1962**, *237*, 3006−3008.
(38) Tomohiro, T.; Morimoto, S.; Shima, T.; Chiba, J.; Hatanaka, Y. An Isotope-Coded Fluorogenic Cross-Linker for High-Performance Target Identification Based on Photoaffinity Labeling. *Angew. Chem., Int. Ed.* **2014**, *53*, 13502−5.
(39) Tomohiro, T.; Yamamoto, A.; Tatsumi, Y.; Hatanaka, Y. [3-(Trifluoromethyl)-3H-diazirin-3-yl]coumarin as a carbene-generating photocross-linker with masked fluorogenic beacon. *Chem. Commun.* **2013**, *49*, 11551−3.
(40) Murale, D. P.; Hong, S. C.; Yun, J.; Yoon, C. N.; Lee, J. S. Rational design of a photo-crosslinking BODIPY for in situ protein labeling. *Chem. Commun.* **2015**, *51*, 6643−6.
(41) Wang, Y.; Hu, L.; Xu, F.; Quan, Q.; Lai, Y.-T.; Xia, W.; Yang, Y.; Chang, Y.-Y.; Yang, X.; Chai, Z.; Wang, J.; Chu, I. K.; Li, H.; Sun, H. Integrative approach for the analysis of the proteome-wide response to bismuth drugs in Helicobacter pylori. *Chem. Sci.* **2017**, *8*, 4626−4633.
(42) Chao, A.; Jiang, N.; Yang, Y.; Li, H.; Sun, H. A Ni-NTA-based red fluorescence probe for protein labelling in live cells. *J. Mater. Chem. B* **2017**, *5*, 1166−1173.
(43) Lai, Y. T.; Chang, Y. Y.; Hu, L.; Yang, Y.; Chao, A.; Du, Z. Y.; Tanner, J. A.; Chye, M. L.; Qian, C.; Ng, K. M.; Li, H.; Sun, H. Rapid labeling of intracellular His-tagged proteins in living cells. *Proc. Natl. Acad. Sci. U. S. A.* **2015**, *112*, 2948−53.
(44) Chiba, K.; Asanuma, M.; Ishikawa, M.; Hashimoto, Y.; Dodo, K.; Sodeoka, M.; Yamaguchi, T. Specific fluorescence labeling of target proteins by using a ligand-4-azidophthalimide conjugate. *Chem. Commun.* **2017**, *53*, 8751−8754.
(45) Tian, Y.; Lin, Q. Genetic encoding of 2-aryl-5-carboxytetrazole-based protein photo-cross-linkers. *Chem. Commun.* **2018**, *54*, 4449−4452.

https://dx.doi.org/10.1021/jacs.0c08068
J. Am. Chem. Soc. 2020, 142, 17156−17166

(46) Tian, Y.; Jacinto, M. P.; Zeng, Y.; Yu, Z.; Qu, J.; Liu, W. R.; Lin, Q. Genetically Encoded 2-Aryl-5-carboxytetrazoles for Site-Selective Protein Photo-Cross-Linking. *J. Am. Chem. Soc.* **2017**, *139*, 6078−6081.
(47) Cheng, K.; Lee, J. S.; Hao, P.; Yao, S. Q.; Ding, K.; Li, Z. Tetrazole-Based Probes for Integrated Phenotypic Screening, Affinity-Based Proteome Profiling, and Sensitive Detection of a Cancer Biomarker. *Angew. Chem., Int. Ed.* **2017**, *56*, 15044−15048.
(48) Zhao, S.; Dai, J.; Hu, M.; Liu, C.; Meng, R.; Liu, X.; Wang, C.; Luo, T. Photo-induced coupling reactions of tetrazoles with carboxylic acids in aqueous solution: application in protein labelling. *Chem. Commun.* **2016**, *52*, 4702−5.
(49) Li, Z.; Qian, L.; Li, L.; Bernhammer, J. C.; Huynh, H. V.; Lee, J. S.; Yao, S. Q. Tetrazole Photoclick Chemistry: Reinvestigating Its Suitability as a Bioorthogonal Reaction and Potential Applications. *Angew. Chem., Int. Ed.* **2016**, *55*, 2002−6.
(50) Herner, A.; Marjanovic, J.; Lewandowski, T.; Marin, V. L.; Patterson, M. J.; Miesbauer, L.; Ready, D.; Williams, J.; Vasudevan, A.; Lin, Q. 2-Aryl-5-carboxytetrazole as a New Photoaffinity Label for Drug Target Identification. *J. Am. Chem. Soc.* **2016**, *138*, 14609−14615.
(51) Ota, E.; Usui, K.; Oonuma, K.; Koshino, H.; Nishiyama, S.; Hirai, G.; Sodeoka, M. Thienyl-Substituted alpha-Ketoamide: A Less Hydrophobic Reactive Group for Photo-Affinity Labeling. *ACS Chem. Biol.* **2018**, *13*, 876−880.
(52) Ankenbruck, N.; Courtney, T.; Naro, Y.; Deiters, A. Optochemical Control of Biological Processes in Cells and Animals. *Angew. Chem., Int. Ed.* **2018**, *57*, 2768−2798.
(53) Sato, S.; Morita, K.; Nakamura, H. Regulation of target protein knockdown and labeling using ligand-directed Ru(bpy)3 photocatalyst. *Bioconjugate Chem.* **2015**, *26*, 250−6.
(54) Sato, S.; Nakamura, H. Ligand-directed selective protein modification based on local single-electron-transfer catalysis. *Angew. Chem., Int. Ed.* **2013**, *52*, 8681−4.
(55) Geri, J. B.; Oakley, J. V.; Reyes-Robles, T.; Wang, T.; McCarver, S. J.; White, C. H.; Rodriguez-Rivera, F. P.; Parker, D. L.; Hett, E. C.; Fadeyi, O. O.; Oslund, R. C.; MacMillan, D. W. C. Microenvironment mapping via Dexter energy transfer on immune cells. *Science* **2020**, *367*, 1091.
(56) Ito, K.; Sawanobori, J. 4-Diazomethyl-7-Methoxycoumarin as a New Type of Stable Aryldiazomethane Reagent. *Synth. Commun.* **1982**, *12*, 665−671.
(57) Takadate, A.; Tahara, T.; Fujino, H.; Goya, S. Synthesis and Properties of 4-Diazomethyl-7-methoxycoumarin as a New Fluorescent Labeling Reagent for Alchohols and Carboxyacids. *Chem. Pharm. Bull.* **1982**, *30*, 4120−4125.
(58) Ito, K.; Maruyama, J. Studies on Stable Diazoalkanes as Potential Fluorogenic Reagents. I. 7-Substituted 4-Diazomethylcoumarins. *Chem. Pharm. Bull.* **1983**, *31*, 3014−3023.
(59) Ito, K.; Maruyama, J. Studies on Stable Diazoalkanes as Potential Fluorogenic Reagents. II.: Ring-Fused 4-Diazomethylcoumarins. *Chem. Pharm. Bull.* **1986**, *34*, 390−395.
(60) Ando, H.; Furuta, T.; Tsien, R. Y.; Okamoto, H. Photo-mediated gene activation using caged RNA/DNA in zebrafish embryos. *Nat. Genet.* **2001**, *28*, 317−25.
(61) Sivakumar, K.; Xie, F.; Cash, B. M.; Long, S.; Barnhill, H. N.; Wang, Q. A Fluorogenic 1,3-Dipolar Cycloaddition Reaction of 3-Azidocoumarins and Acetylenes. *Org. Lett.* **2004**, *6*, 4603−4606.
(62) Bethell, D.; Stevens, G.; Tickle, P. The reaction of diphenylmethylene with isopropyl alcohol and oxygen: the question of reversibility of singlet-triplet interconversion of carbenes. *J. Chem. Soc. D* **1970**, *0*, 792b−794.
(63) Dean, F. M.; Park, B. K. Activating groups for the ring expansion of coumarin by diazoethane: benzoyl, pivaloyl, arylsulphonyl, arylsulphinyl, and nitro. *J. Chem. Soc., Perkin Trans. 1* **1976**, 1260−1268.
(64) McMahon, R. J.; Abelt, C. J.; Chapman, O. L.; Johnson, J. W.; Kreil, C. L.; LeRoux, J. P.; Mooring, A. M.; West, P. R. 1,2,4,6-Cycloheptatetraene: the key intermediate in arylcarbene interconversions and related C7H6 rearrangements. *J. Am. Chem. Soc.* **1987**, *109*, 2456−2469.
(65) Dubinsky, L.; Krom, B. P.; Meijler, M. M. Diazirine based photoaffinity labeling. *Bioorg. Med. Chem.* **2012**, *20*, 554−70.
(66) Ito, K.; Maruyama, J. A Facile Intramolecular Cyclization of 4-Diazomethylcoumarins. A Convenient Route to Benzopyrano[3,4-c]pyrazol-4(3H)-ones. *Heterocycles* **1984**, *22*, 1057−1059.
(67) Preston, G. W.; Wilson, A. J. Photo-induced covalent cross-linking for the analysis of biomolecular interactions. *Chem. Soc. Rev.* **2013**, *42*, 3289−3301.
(68) Takagaki, Y.; Gupta, C. M.; Khorana, H. G. Thiols and the diazo group in photoaffinity labels. *Biochem. Biophys. Res. Commun.* **1980**, *95*, 589−595.
(69) McGrath, N. A.; Andersen, K. A.; Davis, A. K.; Lomax, J. E.; Raines, R. T. Diazo compounds for the bioreversible esterification of proteins. *Chem. Sci.* **2015**, *6*, 752−755.
(70) Teruya, K.; Tonissen, K. F.; Poulsen, S.-A. Recent developments of small molecule chemical probes for fluorescence-based detection of human carbonic anhydrase II and IX. *MedChemComm* **2016**, *7*, 2045−2062.
(71) Supuran, C. T. How many carbonic anhydrase inhibition mechanisms exist? *J. Enzyme Inhib. Med. Chem.* **2016**, *31*, 345−60.
(72) Li, G.; Liu, Y.; Liu, Y.; Chen, L.; Wu, S.; Liu, Y.; Li, X. Photoaffinity labeling of small-molecule-binding proteins by DNA-templated chemistry. *Angew. Chem., Int. Ed.* **2013**, *52*, 9544−9.
(73) Mallory, J. C.; Crudden, G.; Oliva, A.; Saunders, C.; Stromberg, A.; Craven, R. J. A novel group of genes regulates susceptibility to antineoplastic drugs in highly tumorigenic breast cancer cells. *Mol. Pharmacol.* **2005**, *68*, 1747−56.
(74) Hulikova, A.; Aveyard, N.; Harris, A. L.; Vaughan-Jones, R. D.; Swietach, P. Intracellular carbonic anhydrase activity sensitizes cancer cell pH signaling to dynamic changes in CO_2 partial pressure. *J. Biol. Chem.* **2014**, *289*, 25418−30.
(75) Supuran, C. T. Carbonic Anhydrases - An Overview. *Curr. Pharm. Des.* **2008**, *14*, 603−614.
(76) Soethoudt, M.; Stolze, S. C.; Westphal, M. V.; van Stralen, L.; Martella, A.; van Rooden, E. J.; Guba, W.; Varga, Z. V.; Deng, H.; van Kasteren, S. I.; Grether, U.; IJzerman, A. P.; Pacher, P.; Carreira, E. M.; Overkleeft, H. S.; Ioan-Facsinay, A.; Heitman, L. H.; van der Stelt, M. Selective Photoaffinity Probe That Enables Assessment of Cannabinoid CB2 Receptor Expression and Ligand Engagement in Human Cells. *J. Am. Chem. Soc.* **2018**, *140*, 6067−6075.
(77) Yang, J.-S.; Lin, C.-W.; Chuang, C.-Y.; Su, S.-C.; Lin, S.-H.; Yang, S.-F. Carbonic anhydrase IX overexpression regulates the migration and progression in oral squamous cell carcinoma. *Tumor Biol.* **2015**, *36*, 9517−9524.
(78) Tafreshi, N. K.; Lloyd, M. C.; Bui, M. M.; Gillies, R. J.; Morse, D. L. Carbonic Anhydrase IX as an Imaging and Therapeutic Target for Tumors and Metastases. In *Carbonic Anhydrase: Mechanism, Regulation, Links to Disease, and Industrial Applications*; Frost, S. C., McKenna, R., Eds.; Springer: Dordrecht, 2014; pp 221−254.
(79) Benej, M.; Pastorekova, S.; Pastorek, J. Carbonic Anhydrase IX: Regulation and Role in Cancer. In *Carbonic Anhydrase: Mechanism, Regulation, Links to Disease, and Industrial Applications*; Frost, S. C., McKenna, R., Eds.; Springer: Dordrecht, 2014; pp 199−219.
(80) An, W. G.; Kanekal, M.; Simon, M. C.; Maltepe, E.; Blagosklonny, M. V.; Neckers, L. M. Stabilization of wild-type p53 by hypoxia-inducible factor 1α. *Nature* **1998**, *392*, 405−408.
(81) Geißler, D.; Antonenko, Y. N.; Schmidt, R.; Keller, S.; Krylova, O. O.; Wiesner, B.; Bendig, J.; Pohl, P.; Hagen, V. Coumarin-4-yl)methyl Esters as Highly Efficient, Ultrafast Phototriggers for Protons and Their Application to Acidifying Membrane Surfaces. *Angew. Chem., Int. Ed.* **2005**, *44*, 1195−1198.
(82) Bort, G.; Gallavardin, T.; Ogden, D.; Dalko, P. I. From one-photon to two-photon probes: "caged" compounds, actuators, and photoswitches. *Angew. Chem., Int. Ed.* **2013**, *52*, 4526−37.
(83) Dyer, J.; Jockusch, S.; Balsanek, V.; Sames, D.; Turro, N. J. Two-Photon Induced Uncaging of a Reactive Intermediate. Multi-

photon In Situ Detection of a Potentially Valuable Label for Biological Applications. *J. Org. Chem.* **2005**, *70*, 2143−2147.
(84) Urdabayev, N. K.; Popik, V. V. Wolff Rearrangement of 2-Diazo-1(2H)-Naphthalenone Induced by Nonresonant Two-Photon Absorption of NIR Radiation. *J. Am. Chem. Soc.* **2004**, *126*, 4058−4059.
(85) Miller, L. W.; Cai, Y.; Sheetz, M. P.; Cornish, V. W. In vivo protein labeling with trimethoprim conjugates: a flexible chemical tag. *Nat. Methods* **2005**, *2*, 255−257.

https://dx.doi.org/10.1021/jacs.0c08068
J. Am. Chem. Soc. 2020, 142, 17156−17166